Available online at www.sciencedirect.com
ScienceDirect
Journal of Power Sources 175 (2008) 625–629
JOURNAL OF POWER SOURCES
www.elsevier.com/locate/jpowsour

Short communication

Nickel oxyhydroxide/manganese dioxide composite as a candidate electrode material for alkaline secondary cells

T.N. Ramesh *, P. Vishnu Kamath

Department of Chemistry, Central College, Bangalore University, Bangalore 560001, India

Received 20 June 2007; received in revised form 27 August 2007; accepted 30 August 2007
Available online 6 September 2007

Abstract

Nickel hydroxide and manganese dioxide are used in alkaline cells as positive electrode materials. Positive electrodes comprising a nickel oxyhydroxide/manganese dioxide composite, with modification by Bi_2O_3, deliver a combined reversible discharge capacity of 2.25e per metal atom (650 mAh g^{-1} metal content), which is higher than that realized from electrodes of either component taken singly. The composite discharges with two potential plateaux, the first appearing at 325 mV corresponds to the discharge of the nickel component, whereas the second at −600 mV is due to the manganese component. Composites of $NiO(OH)/MnO_2$ can be used as a new electrode material with higher discharge capacity than conventional electrodes.

Keywords: Nickel hydroxide; Manganese dioxide; Nickel oxyhydroxide/manganese dioxide composite; Electrode material

1. Introduction

Divalent metal hydroxides and trivalent metal oxide–hydroxides crystallize in a structure related to that of the mineral brucite, $Mg(OH)_2$ [1]. Brucite is comprised of a hexagonal close packing of hydroxyl ions with alternative layers of octahedral sites occupied by divalent metal ions. This results in the stacking of charge-neutral layers of the composition $[M(OH)_2]$ (M = divalent metal), with an interlayer spacing of 4.6 Å [2].

When the M^{2+} is partially or completely oxidized to the 3+ state, an equivalent number of protons are eliminated from $M(OH)_2$ to restore charge neutrality and results in a composition MO(OH) [3]. On account of their facile and reversible proton intercalation, the hydroxides of Ni^{2+} and Co^{2+} are good electrode materials for alkaline secondary cells [4].

Manganese dioxide is also used as an electrode material in alkaline batteries. Generally, λ-manganese dioxide crystallizes with a three-dimensional rutile structure [5]. By contrast, anodic oxidation of $Mn(CH_3COO)_2$ or $MnSO_4$, leads to the formation of a manganese dioxide designated as electrolytic γ-MnO_2 (EMD). Also the products obtained by the oxidation of manganese(II) salts using hydrogen peroxide crystallize in a layered structure, whose mineral form is known as birnessite (δ-MnO_2) [6]. Given the close structural relationship between $M(OH)_2$ and birnessite-type MO_2, a common reaction scheme was proposed for the charge–discharge process of the oxide/hydroxide electrodes [7]:

$$\underset{\text{divalent hydroxide}}{M^{II}(OH)_2} \overset{a}{\underset{d}{\Leftrightarrow}} \underset{\text{trivalent bronze}}{H^{III}MO_2} \overset{b}{\underset{c}{\Leftrightarrow}} \underset{\text{quadrivalent dioxide}}{M^{IV}O_2}$$

where M = Ni, Co and Mn.

This scheme provides an opportunity to explore the possibility of a 2e exchange in an ideal electrode material. Earlier work has indeed demonstrated the exchange of nearly 1.7e in the nickel hydroxide electrode [8,9] and 2e exchange in MnO_2 [10]. Conventionally, the charge–discharge process of $Ni(OH)_2$ is represented by steps a/d. MnO_2 discharges reversibly by steps b/c if the discharge is limited to 0.3e in step (c) [11]. MnO(OH) is unstable as Mn^{3+} is a Jahn–Teller ion and therefore on deeper discharge the insulating Mn_3O_4 spinel phase is formed [12]:

$$MnO_2 \Leftrightarrow MnO(OH) \rightarrow Mn_3O_4$$

Wroblowa and Gupta [13] blended a small amount of Bi_2O_3 in manganese oxide during electrode fabrication to induce

* Corresponding author. Tel.: +91 80 22961354.
E-mail address: rameshtn77@yahoo.co.in (T.N. Ramesh).

0378-7753/$ – see front matter © 2007 Elsevier B.V. All rights reserved.
doi:10.1016/j.jpowsour.2007.08.097

reversibility up to deeper levels of discharge in manganese dioxide.

Nickel hydroxide has limitations arising from the high rate of self-discharge and low volumetric energy density [14]. MnO_2, on the other hand, has a negative charge discharge potential plateau. A combination of these two electrode materials would in principle lead to an electrode superior to those obtained from each separately.

Mineral asbolane is an intergrowth of MnO_2, $Ni(OH)_2$ and $CoO(OH)/Co(OH)_3$ [15]. Nickel hydroxide–MnO_2 compounds with a mixed layered structure have been synthesized by inserting nickel hydroxide into layered MnO_2 under hydrothermal conditions [16].

Asbolane inspired us to explore the possible utilization of the combined electrochemical properties of MnO_2 and $Ni(OH)_2$ in a single electrode material. Nickel hydroxide has a positive discharge plateau in the potential range of 0.350–0.30 V with respect to $Hg/HgO/OH^-$ [17]. MnO_2 electrodes exhibit two discharge plateaux at a negative potential of −0.2 to 0.3 V and around −0.6 to 0.8 V with respect to $Hg/HgO/OH^-$, respectively [18]. In the positive potential range up to 0 mV, nickel hydroxide works as an active material and once it is completely discharged MnO_2 starts to discharge. This paper reports the discharge capacity of $NiO(OH)/MnO_2$ composite electrodes. When Bi_2O_3 is incorporated as an additive in the composite during electrode fabrication, the discharge capacity increased from 187 mAh g^{-1} to 980 mAh g^{-1} of Mn in the MnO_2 region.

2. Experimental

β_{bc}-Nickel hydroxide was obtained as described elsewhere [17] by adding a nickel nitrate solution (1 M, 50 mL) to NaOH (2 M, 100 mL) at 80 °C under constant stirring. The green slurry was aged in mother liquor for 18 h at 80 °C. The precipitate was filtered, washed free of alkali, and dried at 65 °C.

MnO_2 was obtained by the sol–gel method [19]. Nine grams of $KMnO_4$ and 15 g of glucose were dissolved in 75 mL of water separately. Both the solutions were mixed together and the mixture was stirred thoroughly for 10 min. The reddish product obtained was allowed to settle. The supernatant was decanted and the semi-solid was calcined at 400 °C for 2 h. The powder was washed with water and dried at 100 °C to constant weight.

Bi_2O_3 was obtained from a commercial source (Loba Chemie, India) and used as such. The $NiO(OH)/MnO_2$ composite was prepared by adding a mixed metal ($Ni^{2+} + Mn^{2+}$) nitrate solution to a solution containing three times excess of NaOH and five times excess of 20% (w/v) of H_2O_2 required for precipitation and oxidation, respectively. The dark brown product was aged in mother liquor for 24 h prior to filtration. The product was washed free of alkali and dried at 80 °C to constant weight.

All samples were characterized by powder X-ray diffraction (PXRD) (Philips X'Pert Pro diffractometer, Cu Kα source, λ = 1.5418 Å, graphite secondary monochromator) and infrared spectroscopy (Nicolet Impact 400D FTIR spectrometer, KBr pellets, 4 cm^{-1} resolution).

2.1. Charge–discharge studies

Galvanostatic charge–discharge studies were carried out using an EG&G Versastat model IIA scanning potentiostat. Electrodes were prepared by mixing the active material with graphite powder and an aqueous suspension of polytetrafluoroethylene in the ratio 0.6:0.3:0.1. The mixtures were ground thoroughly to obtain a paste-like consistency. This paste was pressed at 75–120 kg cm^{-2} on both sides of a nickel foam (2.9 cm × 2.3 cm) support at the ambient temperature of 25–30 °C.

In case of physically modified electrodes, different proportions (5, 10 and 24.8 wt.%) of Bi_2O_3 were added to the active material. An electrode comprising Bi_2O_3 in place of the active material was also cycled to investigate its contribution, if any, to the charge-storage capacity. All the electrodes were dried at 65 °C and soaked in 6 M KOH for 24 h before being galvanostatically charged at ∼5.5 mA to 120% of the theoretical capacity computed for a 1e exchange in case of nickel hydroxide and 150% of the theoretical capacity computed for a 3e exchange in case of nickel hydroxide–manganese dioxide composites. Nickel plates were used as counter electrodes, and all potentials were measured against a $Hg/HgO/OH^-$ (6 M KOH) reference electrode.

For β_{bc}-nickel hydroxide the cut-off voltage is 0 mV, whereas for other electrodes such as manganese dioxide, Bi_2O_3 doped manganese dioxide, $NiO(OH)/MnO_2$ composite and Bi_2O_3 doped $NiO(OH)/MnO_2$ electrodes, the cut-off voltage is −800 mV. These electrodes were then discharged at a current of 20 mA to their respective discharge potentials mentioned above at the ambient temperature (25–28 °C). The observed capacities were normalized to the metal content.

3. Results and discussion

As-prepared nickel hydroxide is in its discharged state, whereas the as-prepared MnO_2 is in its charged state. A physical mixture of these two materials is not ready for use in charge-storage applications. We therefore coprecipitated both Ni^{2+} and Mn^{2+} under oxidizing conditions at high pH to obtain a composite of NiO(OH) and MnO_2. The PXRD patterns of $Ni(OH)_2$, MnO_2 and $NiO(OH)/MnO_2$ composite are compared in Fig. 1. The reflections in the PXRD pattern of nickel hydroxide can be indexed to that of β-$Ni(OH)_2$ (PDF: 14-117; $P\bar{3}m1$; $a = 3.01$ Å; $c = 4.67$ Å), whereas the reflections of manganese dioxide exhibit two successive basal reflections at 7.06 and 3.52 Å, which are characteristic of a layered structure. All the reflections of $Ni(OH)_2$, as well as of MnO_2, are considerably broadened due to structural disorder and such disorder facilitates superior charge-storage capacity [20,21]. The basal spacing of the MnO_2 phase (7.06 Å) is much larger than that in $Ni(OH)_2$ (4.6 Å), which indicates the presence of intercalated water in the former. The reflections in the PXRD pattern of composite material do not match with those of either constituent (see Fig. 1). The first reflection appearing at 7.7 Å is higher than the basal spacing of MnO_2 (see Fig. 1). The second reflection, which appears at 4.68 Å close to the (0 0 1) reflection of $Ni(OH)_2$, is actually due

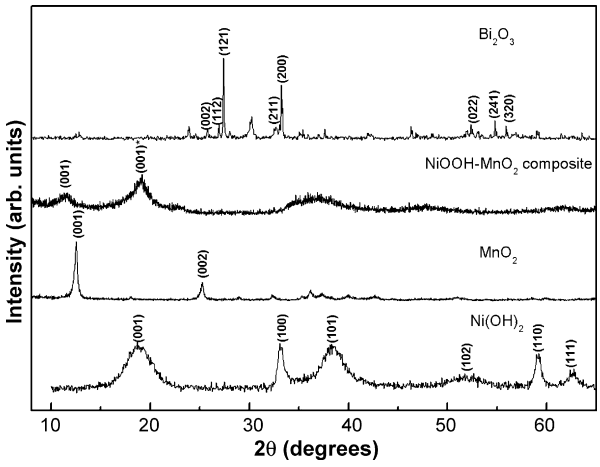

Fig. 1. PXRD patterns of β_{bc} nickel hydroxide, δ-manganese dioxide, nickel oxyhydroxide/manganese dioxide composite, commercial δ-Bi_2O_3, respectively.

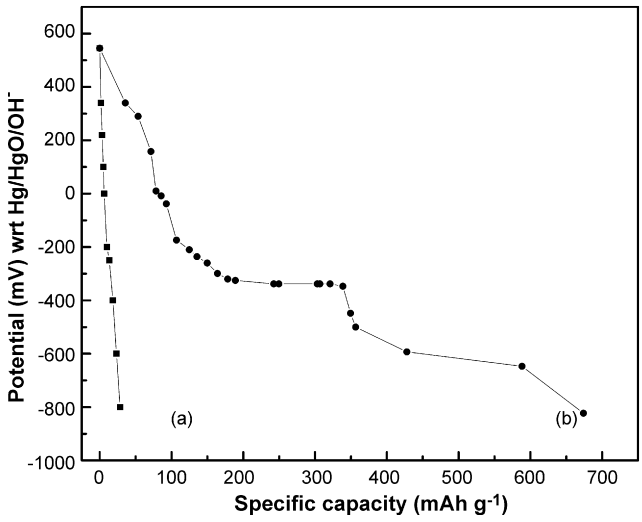

Fig. 3. Discharge curves of (a) δ-manganese dioxide and (b) first discharge curve of δ-manganese dioxide with 24.8 wt.% Bi_2O_3.

to the NiO(OH) phase. The other reflections of NiO(OH) are extinguished. These observations suggest that there is an intimate interaction between the two materials and the composite is not merely a physical mixture of the two phases.

The discharge curve of a nickel hydroxide electrode is presented in Fig. 2(a). The electrode exhibits a single discharge plateau at 325–350 mV. The reversible discharge capacity corresponds to an exchange of 0.8e per Ni atom (350 mAh g^{-1} Ni). This is in keeping with earlier literature data [22]. By contrast, the MnO_2 electrode discharges rapidly with a negligible discharge capacity of <0.1e per Mn atom (40 mAh g^{-1} of Mn) (see Fig. 3(a)). The discharge capacity remains low on cycling, which shows that the MnO_2 electrode has poor reversibility (see Fig. 4(a)).

Lavela et al. [23] have reported the electrochemical behaviour of $LiMn_2O_4$ in lithium batteries. Substitution of Ni^{2+} ion for Li^+ ion in $LiMn_2O_4$, generates a $Ni_xMn_yO_z$ composite. This composite has better structural stability, electrochemical activity, Li^+ ion diffusion coefficient and capacity retention compared with $LiMn_2O_4$. The NiOOH/MnO_2 composite material prepared here should display two distinct plateaux in its discharge curve. The observed discharge curve exhibits the first plateau at 300 mV due to the nickel component. The second plateau appearing at a negative potential of −600 mV due to the Mn component is, however, a very brief characteristic of the poor charge-storage capacity of MnO_2 (see Fig. 5(a)). The capacity of the Ni component at 0.8e per Ni is unaffected. These observations show that although the two materials in the composite interact very intimately, and thereby affect the structure, their electrochemical properties are not altered. This indicates that the redox properties of the cations are determined more by local bonding, such as that within the first coordination sphere, than by the overall long-range structure. The total capacity is 0.95e per Ni + 0.2e per Mn (215 mAh g^{-1} of total metal content) (see Fig. 6(a)). This result is in contrast to the electrochemical behaviour of the $Ni_xMn_yO_z$ composite in lithium batteries [23].

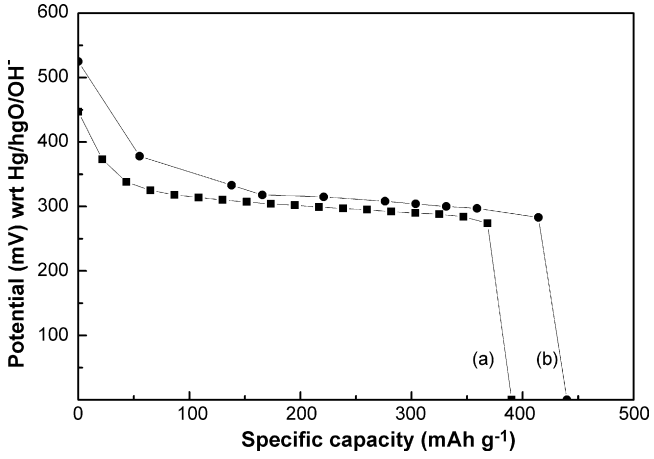

Fig. 2. Discharge curves of (a) nickel hydroxide and (b) nickel hydroxide with 24.8 wt.% Bi_2O_3.

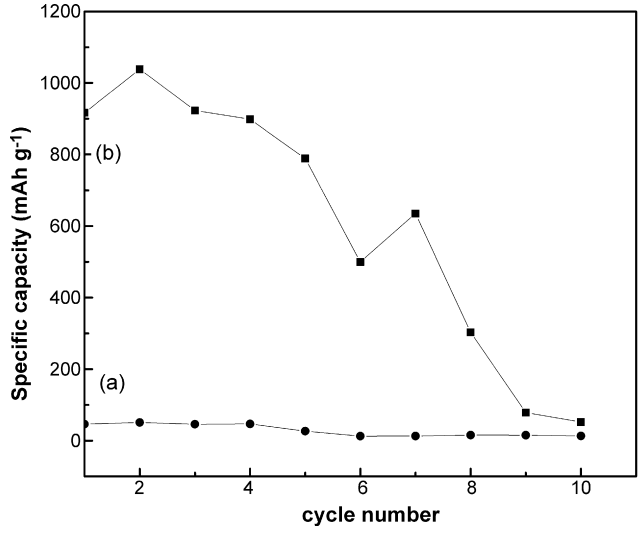

Fig. 4. Cycle-life data of (a) δ-manganese dioxide and (b) δ-manganese dioxide with 24.8 wt.% Bi_2O_3.

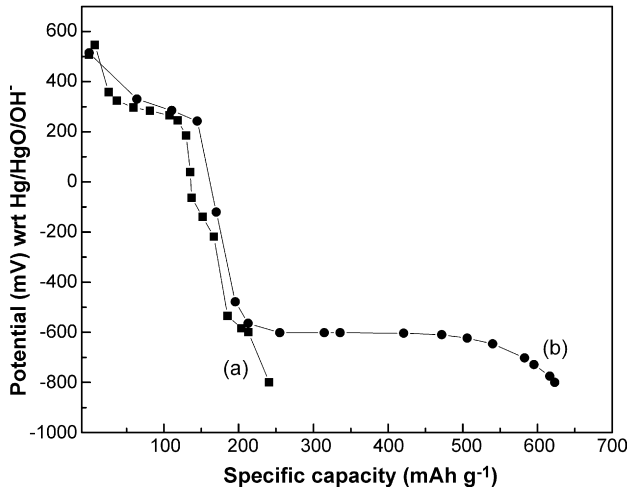

Fig. 5. Discharge curves of (a) nickel oxyhydroxide–manganese dioxide electrode and (b) (a) with 24.8 wt.% Bi_2O_3.

To improve the capacity of the Mn component, Bi_2O_3 was added during electrode fabrication. The PXRD pattern of the Bi_2O_3 sourced commercially is shown in Fig. 1; it corresponds to the α-modification. The beneficial effect of Bi_2O_3 on the MnO_2 component has been well documented in the literature [24–26]. The effect of Bi_2O_3 on the performance of the nickel hydroxide electrode has not, however, been investigated. The effect of mixing different proportions of Bi_2O_3 on the nickel hydroxide electrode is presented in Fig. 7. The cycle-life data of pure Bi_2O_3 exhibits negligible capacity (<40 mAh g^{-1}; <0.05e per Bi_2O_3), see Fig. 7(a). On blending with nickel hydroxide at 5–10 wt.%, the capacity of the nickel hydroxide electrode is adversely affected and comes down to 0.6e per Ni (300 mAh g^{-1} of Ni). At 24.8 wt.% Bi_2O_3, the reversible discharge capacity is restored to that of the pristine electrode. The corresponding cycle-life data are shown in Fig. 7(b–d).

24.8 wt.% Bi_2O_3 added to the pure MnO_2 electrode has a dramatic effect (see Fig. 3(b)). Not only is the discharge plateau in the potential range −300 to −600 mV extended but also the reversibility as shown by the cycle-life data improves and significant capacity (>500 mAh g^{-1} of Mn) is observed up to

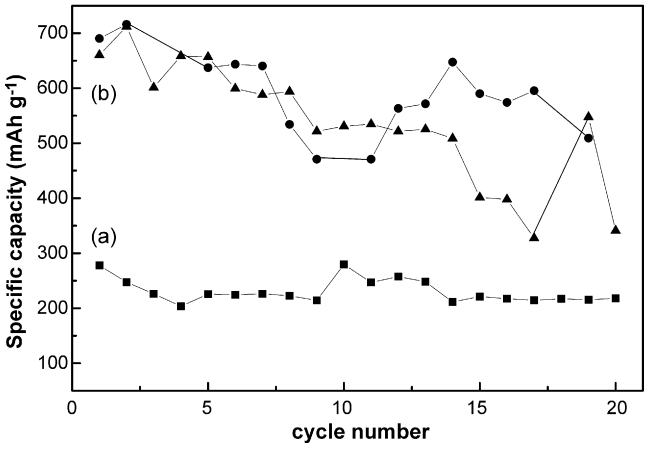

Fig. 6. Cycle-life data of (a) nickel oxyhydroxide–manganese dioxide electrode and (b) (a) with 24.8 wt.% Bi_2O_3.

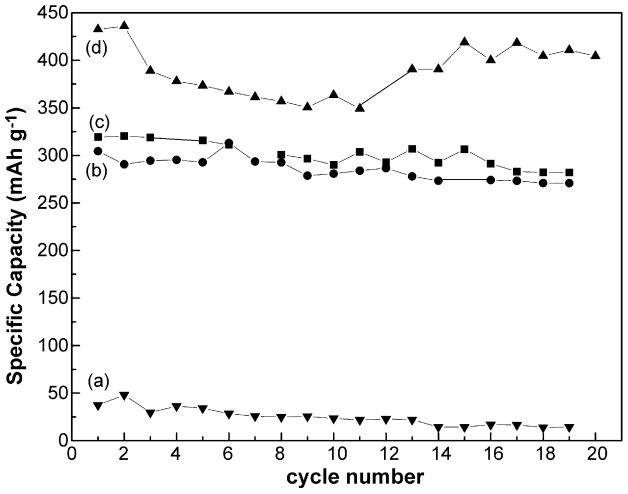

Fig. 7. Cycle-life data of (a) plain Bi_2O_3 electrode and nickel hydroxide electrodes modified with (b) 5 wt.%, (c) 10 wt.% and (d) 24.8 wt.% of Bi_2O_3.

the 7th cycle (see Fig. 4(b)). When Bi_2O_3 is added to the NiO(OH)/MnO_2 composite, the best combined activity of the Ni and Mn components is realized with a combined capacity of 0.95e per Ni + 1.4e per Mn (≈650 mAh g^{-1} of metal) [27]. This value is higher than that obtained from either material taken singly. The cycle-life data are displayed in Fig. 6(b). Two distinct discharge plateaux are observed (see Fig. 5(b)).

4. Conclusion

When compared with nickel hydroxide and manganese dioxide taken singly, the nickel oxyhydroxide/manganese dioxide composite promises to be a new candidate electrode material for alkaline secondary cells.

Acknowledgements

TNR thanks Council of Scientific and Industrial Research (CSIR), Government of India (GOI) for the award of a Senior Research Fellowship (NET). PVK is grateful to the Department of Science and Technology, GOI for financial support and the award of the Ramanna Fellowship. The authors thank Solid State and Structural Chemistry Unit, Indian Institute of Science for providing powder X-ray diffraction facilities.

References

[1] H.R. Oswald, R. Asper, in: R.M.A. Lieth (Ed.), Preparation and Crystal Growth of Materials with Layered Structures, vol. 1, D. Reidel Publishing Co., Dordrecht, 1977, p. 71.
[2] A.F. Wells, Structural Inorganic Chemistry, Oxford University Press, Oxford, 1979.
[3] H. Bode, K. Dehmelt, J. Witte, Electrochim. Acta 11 (1966) 1079.
[4] S.U. Falk, A.J. Salkind, Alkaline Storage Batteries, Wiley, New York, 1969.
[5] A.A. Bolzan, C. Fong, B.J. Kennedy, C.J. Howard, Aust. J. Chem. 46 (1993) 939.
[6] R. Giovanoli, E. Stahli, W. Feitknecht, Helv. Chim. Acta 53 (1970) 453.
[7] J. Ismail, M.F. Ahmed, P.V. Kamath, J. Power Sources 36 (1991) 507.
[8] D.A. Corrigan, S.L. Knight, J. Electrochem. Soc. 136 (1989) 613.

[9] P.V. Kamath, M. Dixit, L. Indira, A.K. Shukla, V.G. Kumar, N. Munichandraiah, J. Electrochem. Soc. 141 (1994) 2956.
[10] J. McBreen, Electrochem. Acta 20 (1975) 221.
[11] K. Kordesch, M. Weissenbacher, J. Power Sources 51 (1994) 61.
[12] J. McBreen, in: D.H. Collins (Ed.), Power Sources, vol. 5, Academic Press, London, 1975, p. 31.
[13] H.S. Wroblowa, N. Gupta, J. Electroanal. Chem. 238 (1987) 93.
[14] M. Kanda, M. Yamamoto, K. Kanno, Y. Satoh, H. Hayashida, M. Suzuki, J. Less-Common Met. 172 (1991) 1227.
[15] A. Manceau, S. Llorca, G. Calas, Geochim. Cosmochim. Acta 51 (1987) 105.
[16] Y. Xu, Q. Feng, K. Kajiyoshi, K. Yanagisawa, X. Yang, Y. Makita, S. Kasaishi, K. Ooi, Chem. Mater. 14 (2002) 3844.
[17] R.S. Jayashree, P.V. Kamath, G.N. Subbanna, J. Electrochem. Soc. 147 (2000) 2029.
[18] D.Y. Qu, J. Appl. Electrochem. 29 (1999) 511.
[19] S. Ching, D.J. Petrovay, M.L. Jorgensen, S.L. Suib, Inorg. Chem. 36 (1997) 883.
[20] A.C. Galliot, V.A. Drits, A. Plancon, B. Lanson, Chem. Mater. 16 (2004) 1890.
[21] C. Tessier, P.H. Haumesser, P. Bernard, C. Delmas, J. Electrochem. Soc. 146 (1999) 2059.
[22] T.N. Ramesh, P.V. Kamath, C. Shivakumara, J. Electrochem. Soc. 152 (2005) 806.
[23] P. Lavela, L. Sanchez, J.L. Tirado, S. Bach, J.P. Pereira-Ramos, J. Power Sources 84 (1999) 75.
[24] D. Qu, D. Hiehl, B.E. Conway, W.G. Pell, S.Y. Qian, J. Appl. Electrochem. 35 (2005) 111.
[25] D.Y. Qu, B.E. Conway, L. Bai, Y.H. Zhou, W.A. Adams, J. Appl. Electrochem. 23 (1993) 693.
[26] R.M. Dell, Phil. Trans. R. Soc. Lond. A 354 (1996) 1515.
[27] X. Xia, Z. Guo, J. Electrochem. Soc. 144 (1997) 213.